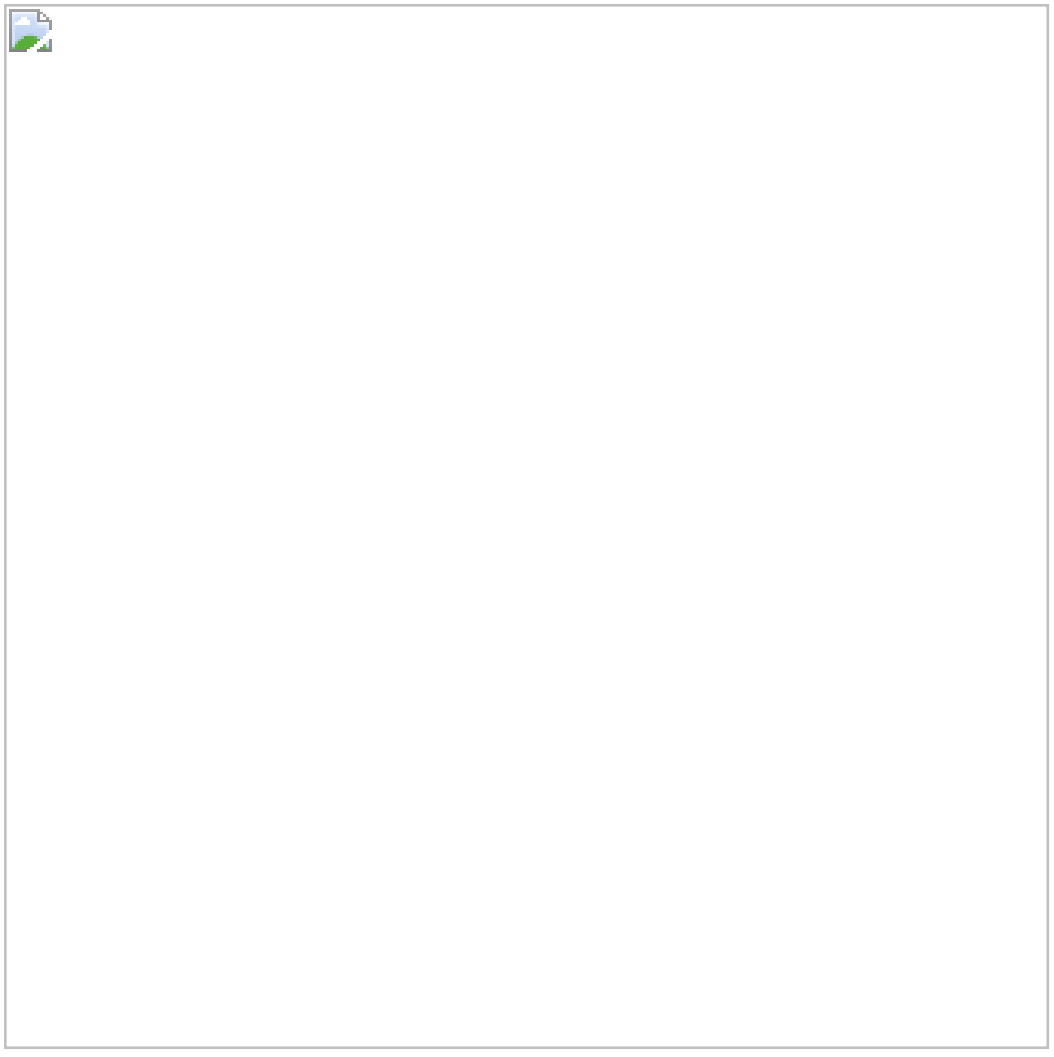

Electromyography of Flight Muscles in Free-Flying Chestnut Tiger Butterfly, Parantica sita

Authors: Ando, Noriyasu, Hirai, Norio, Iima, Makoto, and Senda, Kei

Source: Zoological Science, 41(6)

Published By: Zoological Society of Japan

URL: https://doi.org/10.2108/zs240039

Electromyography of Flight Muscles in Free-Flying Chestnut Tiger Butterfly, *Parantica sita*

Noriyasu Ando[1]*, Norio Hirai[2], Makoto Iima[3], and Kei Senda[4]

[1]*Department of Life Engineering, Faculty of Engineering, Maebashi Institute of Technology, Maebashi, Gunma 371-0816, Japan*
[2]*Department of Environmental Sciences and Technology, Graduate School of Agriculture, Osaka Metropolitan University, Sakai, Osaka 599-8531, Japan*
[3]*Graduate School of Integrated Sciences for Life, Hiroshima University, Higashi-Hiroshima, Hiroshima 739-8521, Japan*
[4]*Department of Aeronautics and Astronautics, Graduate School of Engineering, Kyoto University, Nishikyo-ku, Kyoto 615-8540, Japan*

The chestnut tiger butterfly, *Parantica sita*, can undertake long-distance migrations. They flap their wings for power flight and hold the wings for gliding; such repertoires of wing movements may be the key to explaining their excellent flight abilities. Measuring flight muscle activity using the electromyogram (EMG) is the first step toward understanding the neuromuscular mechanism of active flight control. Free-flight EMG measurements have, however, not been reported in butterflies. This study developed a method to acquire two-channel EMGs from free-flying *P. sita*. Stable EMG recordings were acquired using a monopolar electrode by attaching a small pre-amplifier to the dorsal mesonotum. The common-mode noise between channels was resolved by inserting a reference electrode into the mesonotum midline. The EMGs of five flight muscles were measured during free-flight and their activation phases were analyzed. The EMGs of all five muscles demonstrated a burst of spikes per stroke cycle, in contrast to the few spikes per cycle in the EMGs of hawkmoths, which would reflect the differences in wing kinematics and flight abilities. Further analyses, combining the technique developed in this study with high-speed videography, will clarify the neuromuscular mechanisms underlying the flight ability of *P. sita*.

Key words: insect flight, butterfly, flight muscle, free-flight, electromyogram

INTRODUCTION

Flapping flights in Lepidoptera are diverse, the wingbeat frequency varying from less than 10 Hz in butterflies to 85 Hz in hummingbird hawkmoths (Dudley, 1990; Hunter, 2007). Lepidopterans have synchronous (neurogenic) flight muscles in which motor neuron activity and muscle contraction correspond to each other (Roeder, 1951). Therefore, parameters of the electromyogram (EMG) in each stroke cycle, including the number of spikes, cycle length, and muscle activation phase in a muscle contraction-relax cycle, determine the power output and wing kinematics (Delcomyn, 1997; Sponberg and Daniel, 2012). The indirect "power" muscles generate wing depression and elevation, which are the fundamental movements of wing flapping. Therefore, their EMG parameters reflect the wingbeat frequency and stroke amplitude (Kammer, 1967; Wang et al., 2008). In contrast, direct muscles, known as "control muscles," modulate wing kinematics such as wing pronation-supination and promotion-remotion movements, and control longitudinal and lateral body movements (Kammer, 1971; Rheuben and Kammer, 1987; Arbas et al., 1993; Ando and Kanzaki, 2004; Wang et al., 2008).

Hawkmoths have represented lepidopterans in the study of insect flights. EMG recordings from the hawkmoth flight muscles show a small number of spikes per wing stroke cycle (Kammer, 1971), which is important to shorten muscle contraction and relaxation times and achieves a high wingbeat frequency (Tu and Daniel, 2004), while multiple EMG spikes per cycle is not effective for increasing work output (Stevenson and Josephson, 1990). The spike timing, not the number of spikes, in a contraction cycle determines the power output of the muscles, thereby controlling its contraction with a limited number of spikes (Sponberg and Daniel, 2012). Putney et al. (2019) recently reported that spike timing plays a more dominant role in motor control than the number of spikes in the direct and indirect flight muscles of hawkmoths.

However, large butterflies and moths that flap their wings at low frequencies may primarily use the number of spikes to control wing flapping. Kammer (1967) recorded flight muscle activity from some large lepidopterans (four Saturniid moth species and the monarch butterfly, *Danaus plexippus*) that

* Corresponding author. E-mail: ando@maebashi-it.ac.jp
doi:10.2108/zs240039

flap at low frequencies (approximately 10 Hz). That study reported that the EMG of the indirect wing depressor muscles demonstrated burst-like trains of spikes per wing stroke, with a correlation between the burst length (the duration of a train of spikes) and wing stroke amplitude. Furthermore, Stevenson and Josephson (1990) reported that double stimulation of a flight muscle generates a larger power output with longer interstimulus intervals if the muscle operates at a lower frequency. The use of spike bursts, the number of activated motor units, and/or the number of motor unit recruitments per cycle is, therefore, a reasonable mechanism to control wing kinematics in large lepidopterans flying at lower wingbeat frequencies. Few studies have, however, focused on the neuromuscular mechanisms of such large lepidopterans.

Some butterflies, particularly large species, can glide by holding their wings as well as flapping them. Such a repertoire of wing movements might be important, especially for long-distance migration in butterflies such as the monarch butterfly, *Danaus plexippus* (Reppert et al., 2016), and the chestnut tiger butterfly, *Parantica sita* (Fukuda, 1991; Hirai and Ishii, 1997; Kanazawa et al., 2015). To understand the neuromuscular mechanisms that govern the repertoires of wing movements, it is important to measure the EMGs of flight muscles during free-flight. The EMG can also be measured under tethered flight conditions in which an insect is supported by a rigid or flexible tether. However, flight muscle activities, wing kinematics, and flight force in tethered flight may not accurately represent those in free-flight (Kutsch and Stevenson, 1981; Sane and Dickinson, 2001; Ando and Kanzaki, 2004). Therefore, measuring EMGs of flight muscles in free-flight is necessary for a comprehensive understanding of butterflies' flight mechanisms from physiology to aerodynamics (Senda et al., 2012a, b; Yokoyama et al., 2013). Free-flight EMG measurements in Lepidoptera have been performed in hawkmoths (*Manduca sexta* or *Agrius convolvuli*) through wiring (Arbas et al., 1993; Fernandez et al., 2012; Hedrick et al., 2017) or wireless transmission (Ando and Kanzaki, 2004; Ando et al., 2002; Wang et al., 2008). Free-flight studies have, however, not been conducted on butterflies to date. Unlike the powerful flight ability of hawkmoths, the light body weight and narrow body of butterflies preclude the loading of additional mass, such as a wireless telemeter (Ando et al., 2002). For this reason, wired transmission of muscle potentials is preferred. This paper reports a methodology for acquiring two-channel EMGs from free-flying *P. sita* with wired transmission. A small and light preamplifier was mounted on the dorsal thorax of the butterfly to reduce the noise caused by electrical and mechanical disturbances in the long wires. The study also revealed the patterns of flight muscle activities in free-flying *P. sita*.

MATERIALS AND METHODS

Experimental animals

Adult *P. sita* that were reared on an artificial diet (Hirai, 2001) were obtained from a laboratory colony at Osaka Metropolitan University, Osaka, Japan. The butterflies were kept in triangular envelopes, stored at 10°C under a 16:8 h light: dark cycle, and fed sucrose water every 2–3 days. Seven male and two female butterflies, aged 1–3 months, were used in the free-flight experiments. The mean body weight was 450 ± 49 mg (mean ± standard deviation [SD], n = 7; we failed to weigh two of nine butterflies), and the mean right forewing length (straight-line distance from the wing base to the wing tip) was 54.9 ± 0.11 mm (n = 9).

Amplifiers

A small preamplifier with unity gain was developed that acted as an impedance buffer (Fig. 1A, B). A dual-channel operational amplifier (TL062, Texas Instruments, Dallas, TX) with a thin-shrink small-outline package (TSSOP) (3 × 6.4 mm, including the pin length) was selected because it is light (37 mg) and fits exactly on the dorsal thorax of *P. sita* (thorax width, ca. 3 mm). The preamplifier is a voltage follower that operates without external components. It was supplied by ± 4.5 V through 800 mm long copper wires (80 μm in diameter). The two recording electrodes were polyurethane-coated copper wires (50 μm in diameter), and the single reference electrode was non-insulated silver wire (100 μm in diameter). The output signals from the preamplifier were sent to the main amplifier through 800-mm-long copper wires (80 μm in diameter). In total, five wires (two for power supply, two for signal output, and one for reference connected to the ground) were connected between the mounted preamplifier and the main amplifier.

The main amplifier comprised an input high-pass filter (cutoff frequency: 79.6 Hz) and an instrumentation amplifier (AD623, Analog Devices, Norwood, MA) with a voltage gain of 92. The output of the main amplifier was converted using an analog-to-digital (AD) converter (PowerLab/8SP, AD Instruments, Dunedin, New Zealand) at a sampling rate of 10 kHz, and stored on a computer.

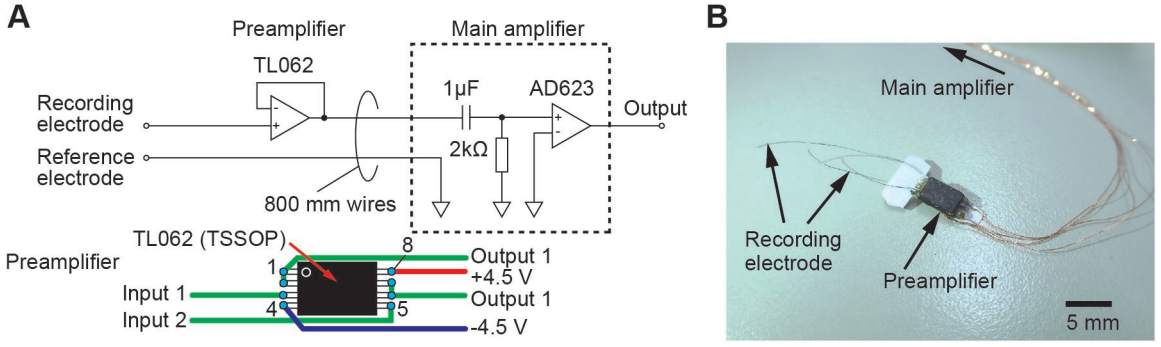

Fig. 1. Onboard preamplifier. **(A)** Circuit diagram and wiring of the preamplifier. The numbers in the wiring diagram indicate pin numbers. Inputs 1 and 2 are recording electrodes. **(B)** Image showing the preamplifier. The reference electrode was separately connected to the main amplifier (not shown).

Animal preparation

Two indirect and three direct muscles (Fig. 2, nomenclature after Ehrlich and Davidson [1961]) were sequentially measured. The dorsal-longitudinal muscles (DLM; muscle numbers 50–54) are indirect wing depressors, and the dorsal-ventral muscles (DVM; muscle numbers 56–59) are indirect wing elevators. The 3rd axillary muscle (3AXM; muscle number 78) is the direct wing retractor muscle. The subalar muscles (SAM; muscle numbers 79 and 80) are direct wing depressors that are also responsible for wing supination, and the basalar muscles (BAM; muscle numbers 69–71) are the direct muscles responsible for wing pronation. The butterflies were fixed on a custom-made setting board and anesthetized using an ice pack placed under the board (Fig. 3A, B). Each recording electrode was inserted into a target muscle through a hole made with the tip of an insect pin (φ 100 μm) after removing the scales on the cuticle. Recording electrodes were inserted from the dorsal surface of the mesonotum for indirect muscle measurements (DLM and DVM), and from the lateral side of the mesothoracic cuticle for direct muscle measurements (3AXM, SAM, and BAM). The reference electrode was inserted into the center of the dorsal mesothorax (Fig. 2B). A reference electrode is usually inserted into the abdomen in EMG recordings of the hawkmoth flight muscles with a monopolar measurement electrode (Ando and Kanzaki, 2004; Ando et al., 2022). This method, however, resulted in a large common-mode signal in both of the recording channels, presumably originating from the abdomen. For a comparison of the EMG signals at different reference electrode positions see Supplementary Text S1 and Supplementary Figure S1. All of the electrodes were fixed with a mixture of beeswax and Canada balsam. After the electrodes were inserted, the preamplifier chip was fixed to the dorsal pronotum using an adhesive (G-18, Konishi, Osaka, Japan) (Fig. 3A, B). A triangular marker consisting of three black points was fixed to the preamplifier chip to monitor the position and orientation of the butterfly during free-flight (Fig. 3C; Ravi et al., 2013). The mass of the preamplifier mounted on the butterfly was 80 mg (including the electrodes and the marker), and the total mass of the device system (preamplifier with the marker, electrodes, and five 800-mm-long wires) was approximately 280 mg. After the preparation, the butterfly was released from the setting board and found to fly freely even with the amplifier mounted.

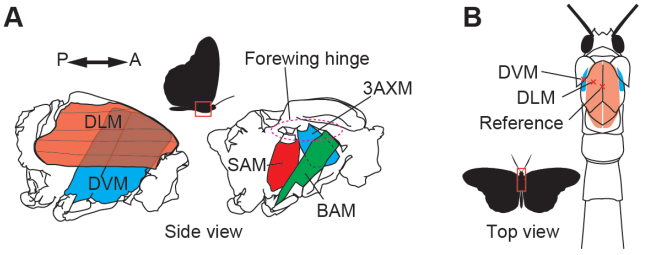

Fig. 2. Flight muscles. **(A)** Flight muscles in the mesothorax. Indirect muscles (DLM and DVM, left) are located in the inner side (on the midline), and direct muscles (3AXM, SAM, and BAM) are located in the outer side, of the thorax. The upper ends of direct muscles attach to the forewing wing hinge (dotted oval). **(B)** The position of the electrodes for measuring indirect power muscles.

Free-flight experiment

A free-flight experiment was conducted in a tunnel without a ceiling, measuring 740 mm (L) × 270 mm (W) × 270 mm (H). Random red squares were displayed on the long sidewalls to guide the forward flight of the butterfly in the tunnel. The red color helped the observers to visually distinguish the wings (black and white) from the background (red and white) from captured video images. The tunnel was illuminated using white LED bulbs (illuminance of 1000 lx). The preamplifier-loaded butterfly was released at the

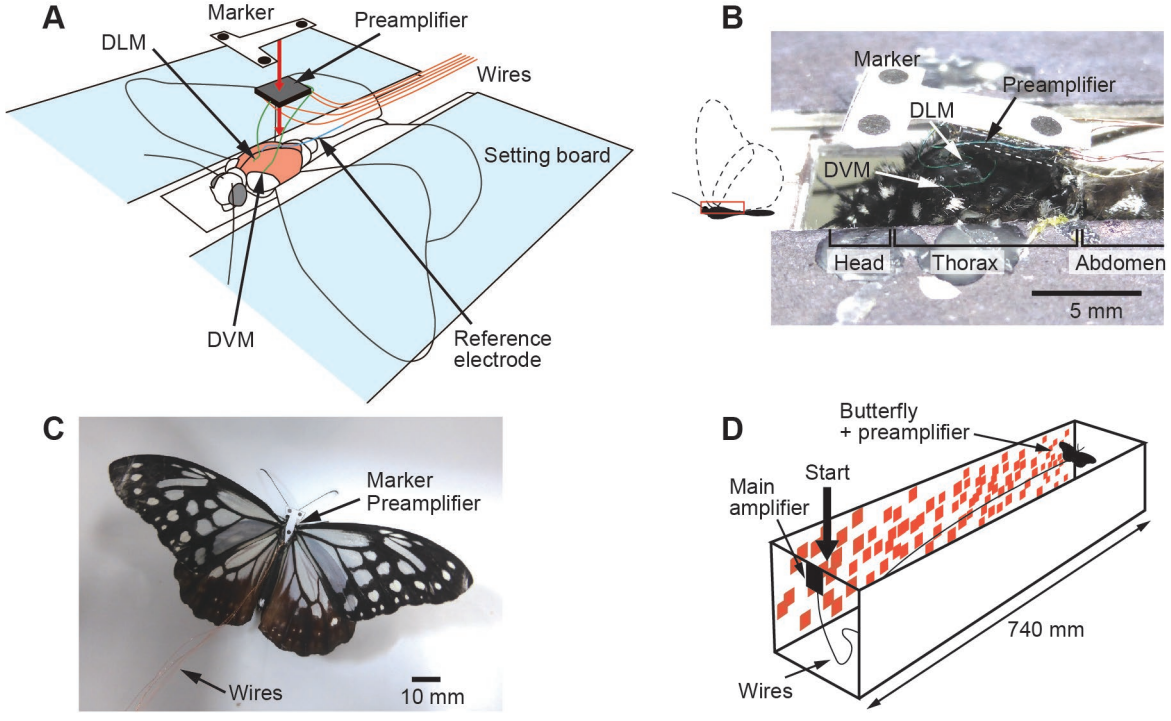

Fig. 3. Animal preparation and experimental conditions. **(A, B)** Animal preparation. The butterfly was fixed on a custom-made setting board, and the preamplifier (surrounded by a dotted square in **[B]**) was fixed on the dorsal thorax. Electrodes were inserted into the DLM and the DVM. **(C)** A preamplifier-loaded butterfly. **(D)** Tunnel for the free-flight experiment. The butterfly was released at the start position and flew forward through the tunnel.

starting point to initiate the flying behavior. It then flew forward until it reached the opposite side (Fig. 3D, and see Supplementary Movie S1). The electrode wires were placed on the arena floor so as not to interfere with the butterflies' free-flight behavior and their lengths were long enough to allow the butterflies to fly freely around the arena. The flying behavior was captured from the top using a digital camera (GoPro HERO5, GoPro, San Mateo, CA) at a frame rate of 240 frames/s. Synchronization between the EMG and video recording was achieved by capturing a blinking LED with the camera and recording the pulse train that illuminated the LED with the AD converter.

Data analysis

To define the wing stroke cycle, the timing of the dorsal stroke reversal (the uppermost position of the wing) was manually detected from the camera images. EMG spikes were detected based on a voltage threshold, followed by the measurement of the time delay of each spike relative to the timing of the dorsal stroke reversal (d). The timing of each EMG spike relative to the cycle length (η) defined as the interval between consecutive dorsal stroke reversals (phase) was calculated as follows:

$$Phase(^\circ) = \frac{d}{\eta} \times 360 \quad (1)$$

All of the analyses were performed using the statistical computing software R (R Core Team, 2022).

Statistics

Circular statistics were employed (R package 'circular'; Agostinelli and Lund, 2023) to characterize the phase of each muscle activity. The Watson-Wheeler test was used to determine the homogeneity of the two sets of circular data. The significance level was set at $P < 0.05$.

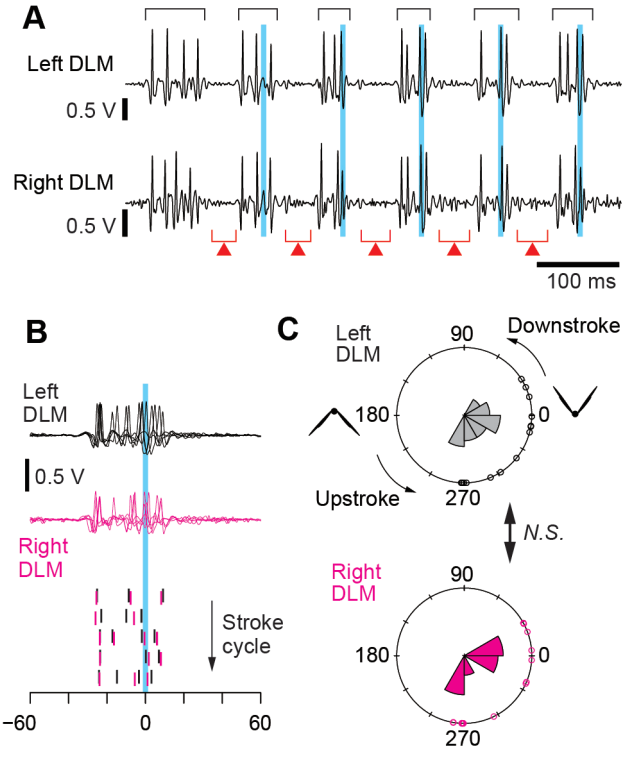

Fig. 4. Bilateral DLM activity during a free-flight. **(A)** EMGs of the bilateral DLM. The cyclic activities of spike bursts (black square brackets) paused by inter-burst intervals (red brackets with triangles) were observed. Blue vertical bars indicate the wing dorsal stroke reversal timing (the uppermost wing position). **(B)** Overlayed DLM spike waveforms and raster plots of DLM spikes detected with thresholds (left and right DLMs are indicated by black and magenta, respectively). The timing of 0 ms indicates the dorsal stroke reversal at each wing stroke. The row of the raster plot indicates the stroke cycle. **(C)** Rose diagrams of the phase of EMG spikes of bilateral DLMs in 4-stroke cycles. The phase of 0° indicates the dorsal stroke reversal (see symbols of wing positions). The radii of the sectors are equal to the square root of the relative number of spikes in a bin of 30°. Plots on a circle indicate the phase of each spike. *P*-values of the Whatson-Wheeler test are shown. *N.S.*, not significant.

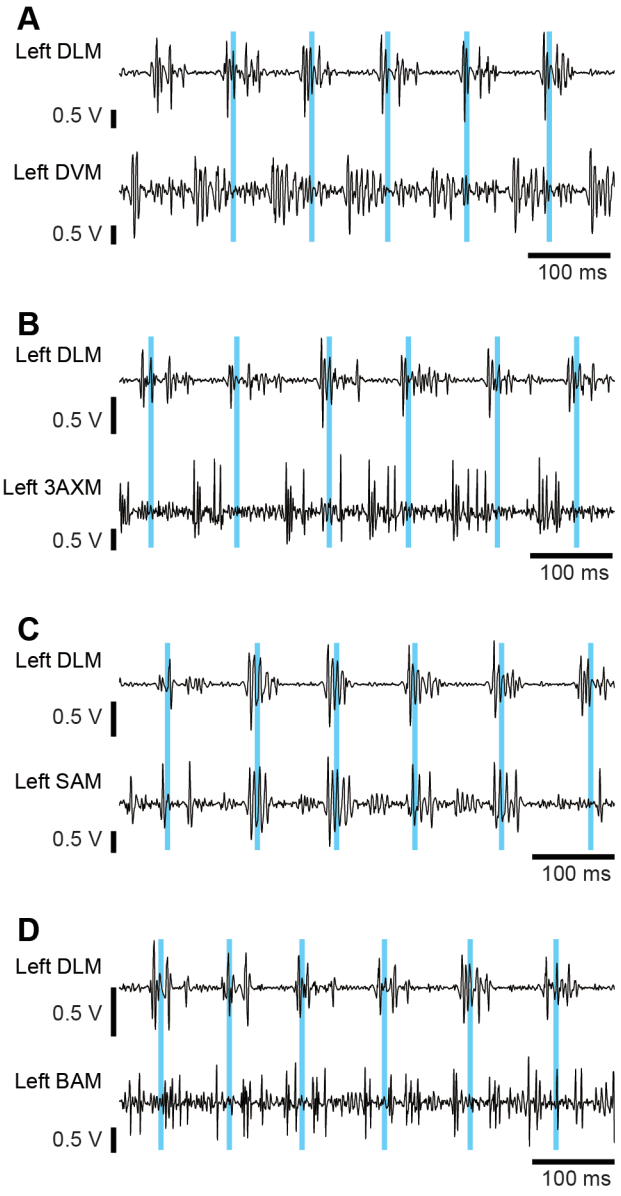

Fig. 5. EMGs of representative flight muscles during a free-flight. **(A–D)** EMGs of the five muscles were measured sequentially in the same butterfly. The DLM activity is shown as a reference. EMGs of the DVM **(A)**, 3AXM **(B)**, SAM **(C)**, and BAM **(D)** are shown. Blue vertical bars indicate the wing dorsal stroke reversal timing. The activation phases of these muscles are shown in Fig. 6.

RESULTS

A total of nine butterflies performed forward flight in the tunnel with the onboard preamplifier and wires, and DLM activity was obtained from all of them. The insertion of the reference electrode into the center of the dorsal thorax (mesonotum midline) effectively reduced the common-mode noise, and rhythmic bursts of spikes were observed in all five muscles. Bilateral DLM recordings demonstrated bursts around the dorsal stroke reversal of the wing and remarkable inter-burst intervals (Fig. 4A), indicating that the contamination of EMG signals from nearby antagonistic muscles such as the DVM was minimized. Furthermore, the raster plots of bilateral DLM spikes (Fig. 4B) indicated that the slight time difference between the left and right DLM spikes was visible although they were active in approximately the same phase (Fig. 4C; no significant difference in phase distribution between left and right DLMs, $P > 0.05$, Watson-Wheeler test). These results indicate that the EMGs of adjacent bilateral muscles could be measured without interference.

Experiments to measure the EMGs of five muscles from the same individual by sequentially changing the position of the electrode were conducted in six butterflies, and all five EMGs were successfully measured from three out of six individuals. Overall, the activities of all five muscles demonstrated bursts of spikes, in contrast with the EMG of hawkmoths (Ando and Kanzaki, 2004; Wang et al., 2008). The position of the DLM recording electrode was fixed throughout the successive measurements; therefore, the difference in DLM waveforms in each measurement would be due to the difference in the recruitment of motor units. The DVM and 3AXM were activated in almost opposite phases to the DLM activity (Figs. 5A, B; 6A, B) whereas the SAM was activated in phase with DLM (Figs. 5C, 6C). In contrast, the BAM was activated throughout the cycle (Figs. 5D, 6D). The phases of EMG spikes in a wing stroke cycle are summarized as rose diagrams in Fig. 6E–H. The DLMs were activated around or slightly before the dorsal stroke reversal (0°). The DVM and 3AXM were activated after the 180° phase, which was an opposite phase of DLM activity, and there were significant differences in the phases between the DLM and DVM, and DLM and 3AXM (Fig. 6E, F; $P < 0.001$, Watson-Wheeler test). On the other hand, the SAM activated almost the same phase as the DLM, with no significant difference observed between them (Fig. 6G, $P > 0.05$). The

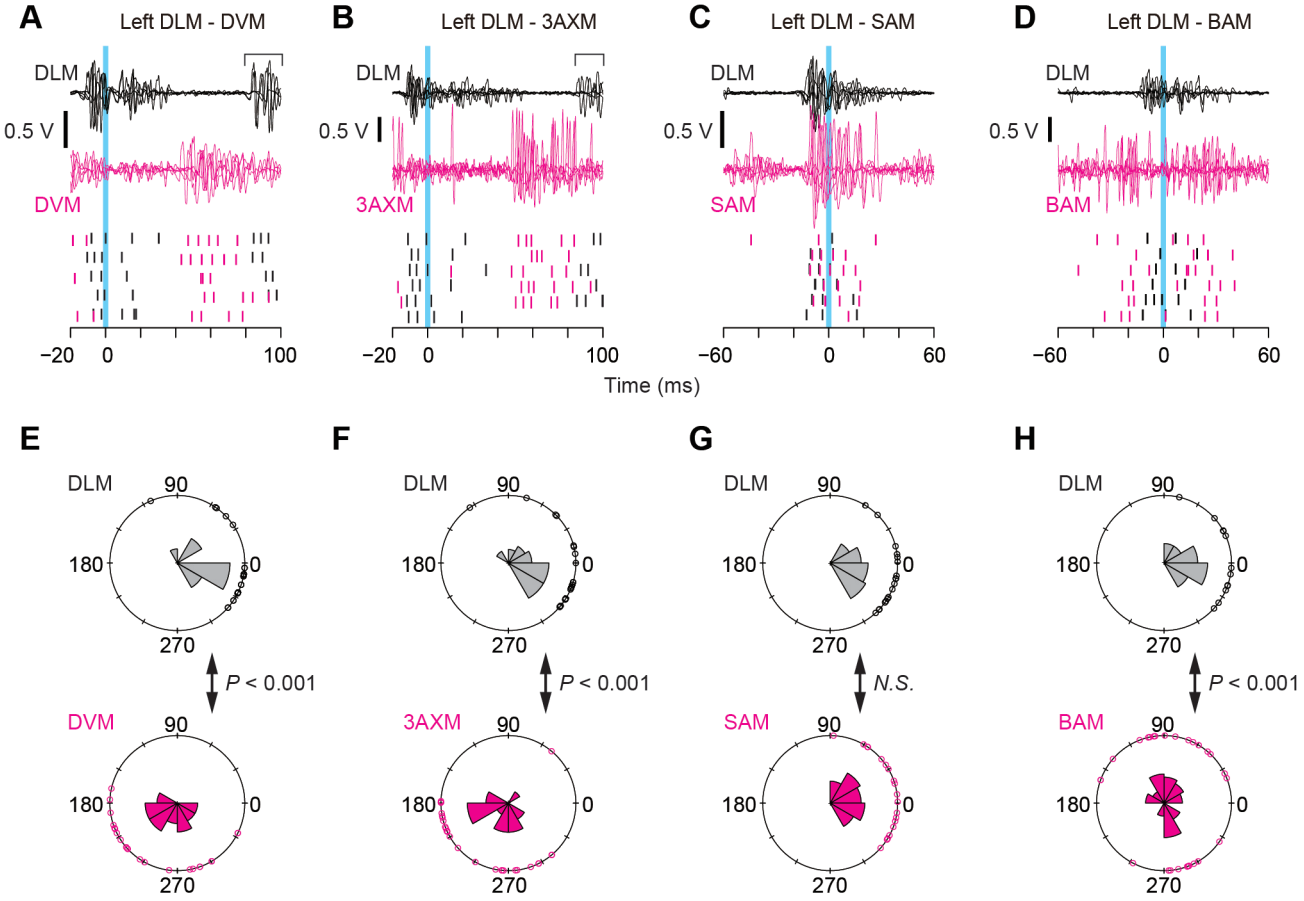

Fig. 6. Timing and phase of EMG spikes relative to stroke cycle. **(A–D)** Overlayed spike waveforms of the EMGs with raster plots of the spikes of the DLM and DVM **(A)**, 3AXM **(B)**, SAM **(C)**, and BAM **(D)**. Descriptions are the same as in Fig. 4B. Waveforms indicated with brackets represent DLM spikes at subsequent wing strokes. **(E–H)** Rose diagrams of the phase of EMG spikes of the DLM and DVM **(E)**, 3AXM **(F)**, SAM **(G)**, and BAM **(H)**. Descriptions are the same as in Fig. 4C. The number of stroke cycles was four for the DVM and five for the 3AXM, SAM, and BAM,. *P*-values of the Whatson-Wheeler test are shown. *N.S.*, not significant.

activation phase of the BAM seemed to be bifurcated around the dorsal stroke reversal (0–180° and 180–360°), and there was a significant difference in the phase between the DLM and BAM (Fig. 6H, $P < 0.001$). These characteristics of the five flight muscles were also observed in two other individuals (see Supplementary Figure S2).

DISCUSSION

This study reports, for the first time, a method for measuring flight muscle activity in free-flying butterflies. This section first discusses the methodology compared to other methods and then the observed characteristics of muscle activity during free-flight.

Wired transmission with long electrode wires is often used to measure muscle activity in free-flying insects. However, long wire-connected muscles and preamplifiers are susceptible to electromagnetic and mechanical interference, resulting in noise in the recorded signals. Differential amplification with bipolar electrodes is an effective solution if this noise is common between electrodes; however, EMG signals were not obtained using long bipolar electrodes with differential amplification in our preparatory experiment (see Supplementary Figure S1A), presumably because of the large mechanical noise generated during free-flight. Loading the amplifier on freely moving animals is advantageous in terms of noise immunity, considering that the length of the electrode can be shortened. This method is broadly used for neural recording in vertebrates (Ewert, 1980) but is not common in small invertebrates such as insects. A limitation of this method is the effect of additional preamplifier weight on the animals. In the case of *P. sita*, the preamplifier (80 mg, including recording electrodes and a marker) weighed approximately 18% of its body weight. The preamplifier is, however, lighter than the wireless telemeter previously used for free-flight EMG measurements in hawkmoths (250 mg, corresponding to 25% of their body weight; Ando et al., 2002). Considering the maximum takeoff weight of butterflies to be twice their body weight as butterflies can fly without hind wings (about half of their wing area) (Jantzen and Eisner, 2008), the added load in this study would be within the butterfly's flight capacity. Although long wires limit the range of insect behavior, EMG recordings are often combined with high-speed camera recordings for kinematic analysis, and the recording range is limited by the field of view of the camera. Furthermore, EMG measurement with a monopolar electrode used in this study is easier to set up and sequentially changes the recorded muscle with minimal invasion of the thoracic tissue compared to differential recording with bipolar electrodes. The key to the successful recording of the flight muscles of a butterfly with a monopolar electrode was the position of the reference electrode at the center of the dorsal thorax (see Supplementary Text S1 and Supplementary Figures S1B–D, S3). Considering these advantages, this method may be applied to flying insects that are lighter and smaller than hawkmoths that cannot carry a wireless transmitter.

The five measured muscles are representative of the study of lepidopteran flight (Kammer, 1967, 1971; Ando and Kanzaki, 2004; Wang et al., 2008; Putney et al., 2019) and this study is the first to present the activation characteristics (phase and bursting) of these representative flight muscles in free-flying butterflies. The overall activation phases of the DVM and SAM were similar to those in tethered and freely flying hawkmoths (Kammer, 1971; Putney et al., 2019; and see Supplementary Figure S4). The SAM is the direct depressor and pronator muscle and its observed synergistic activity with DLM near dorsal stroke reversal suggests that the SAM supports wing depression and adjusts the angle of attack of the wing at the start of wing downstroke. The 3AXM in hawkmoths activates nearly the same phase as the downstroke muscles during tethered flight (Rheuben and Kammer, 1987; Putney et al., 2019). It is, however, antagonistically activated to the downstroke muscle during free-flight (Ando and Kanzaki, 2004; Wang et al., 2008; and see Supplementary Figure S4), which is consistent with our study in butterflies, suggesting that the wing retraction by the 3AXM occurs during upstroke in lepidopterans. The biphasic activity of the BAM was characteristic and was not observed in the other four muscles. Kammer (1971) reported that the BAM of a tethered-flying hawkmoth is activated in multiple phases and concluded that the BAM activity is loosely coupled with the DLM activity. The wings are strongly pronated during dorsal stroke reversal (Dudley, 2000); therefore, the biphasic activity of the BAM before and after the stroke reversal may indicate a continuous adjustment of the wing angle of attack. More detailed measurements are needed to clarify this characteristic biphasic activity pattern to determine whether this is due to differences in the motor units of multiple muscle bundles or to repetitive activity of the same motor units. Electrical stimulation to the muscles is also helpful in identifying the activity and the function of each motor unit.

The bursting activity of muscles per stroke cycle in *P. sata* was a characteristic feature compared to a few spikes per cycle in hawkmoths (Ando and Kanzaki, 2004; Wang et al., 2008). *Parantica sata* flaps at a relatively low frequency (ca. 10 Hz) compared to hawkmoths (ca. 25 Hz for *M. sexta* and 35 Hz for *A. convolvuli*), allowing sufficient time to modulate wing kinematics by accumulating muscle contraction by each spike. If this control strategy differs from that of the hawkmoth (Putney et al., 2019), the flapping mechanism of butterflies is worth elucidating to understand the diversity of lepidopteran flights. Combining our free-flight EMG measurements with kinematic analyses, including wing kinematics and body orientation tracked by the onboard marker, could explain the neuromuscular basis of the long-range flying ability of *P. sita*.

ACKNOWLEDGMENTS

This work was supported by the Japan Society for the Promotion of Science KAKENHI (Grant Number 16H04303 for KS, 20K06743 and 23K05854 for NA) and the SECOM Science and Technology Foundation to KS.

COMPETING INTERESTS

The authors declare that there are no competing interests.

AUTHOR CONTRIBUTIONS

Conceptualization: NA, NH, MI, and KS; Methodology: NA; Formal analysis: NA; Resources: NA and NH; Investigation: NA; Writing—original draft: NA; Writing—review and editing: NA, NH, MI, and KS; Funding acquisition: KS.

SUPPLEMENTARY MATERIALS

Supplementary materials for this article are available online. (URL: https://doi.org/10.2108/zs240039)

Supplementary Text S1. Effectiveness of the preamplifier attachment to the butterfly and reference electrode location for successful monopolar recording of butterfly flight muscles.

Supplementary Figure S1. EMG measurements during free-flight at different amplifier positions and reference electrode positions.

Supplementary Figure S2. EMGs of the five flight muscles during free-flight.

Supplementary Figure S3. Common-mode noise in EMG.

Supplementary Figure S4. Free-flight EMG measurement of the hawkmoth (*Agrius convolvuli*) with a wireless telemeter.

Supplementary Movie S1. Free forward flight of a butterfly with a preamplifier.

REFERENCES

Agostinelli C, Lund U (2023) R package 'circular': Circular Statistics (version 0.5-0). URL: https://CRAN.R-project.org/package=circular / Accessed 17 March 2024

Ando N, Kanzaki R (2004) Changing motor patterns of the 3rd axillary muscle activities associated with longitudinal control in freely flying hawkmoths. Zool Sci 21: 123–130

Ando N, Shimoyama, I, Kanzaki R (2002) A dual-channel FM transmitter for acquisition of flight muscle activities from the freely flying hawkmoth, *Agrius convolvuli*. J Neurosci Methods 115: 181–187

Arbas EA, Willis MA, Kanzaki R (1993) Organization of goal-oriented locomotion: pheromone-modulated flight behavior of moths. In "Biological Neural Networks in Invertebrate Neuroethology and Robotics" Ed by RD Beer, RE Ritzmann, T McKenna, Academic Press, San Diego, pp 159–198

Delcomyn F (1997) Foundations of Neurobiology. W. H. Freeman and Company, New York

Dudley R (1990) Biomechanics of flight in neotropical butterflies: morphometrics and kinematics. J Exp Biol 150: 37–53

Dudley R (2000) The Biomechanics of Insect Flight. Form, Function, and Evolution. Princeton University Press, Princeton

Ehrlich PR, Davidson SE (1961) The internal anatomy of the monarch butterfly, *Danaus plexippus* L. (Lepidoptera: Nymphalidae). Microentomology 24: 85–133

Ewert JP (1980) Neuroethology: An Introduction to the Neurophysiological Fundamentals of Behavior. Springer-Verlag, Berlin, Heidelberg, New York

Fernandez MJ, Springthorpe D, Hedrick TL (2012) Neuromuscular and biomechanical compensation for wing asymmetry in insect hovering flight. J Exp Biol 215: 3631–3638

Fukuda H (1991) Seasonal migration of the chestnut tiger, *Parantica sita* in Japan. Insectarium 28: 4–13

Hedrick TL, Martinez-Blat J, Goodman MJ (2017) Flight motor modulation with speed in the hawkmoth *Manduca sexta*. J Insect Physiol 96: 115–121

Hirai N (2001) Rearing larvae of the chestnut tiger butterfly, *Parantica sita* Koller (Lepidoptera : Danaidae), on artificial Diet. Trans Lepid Soc Japan 52: 109–113

Hirai N, Ishii M (1997) Seasonal occurrence of the chestnut tiger butterfly, *Parantica sita* (Lepidoptera: Danaidae), at 3 habitats in the Kii Peninsula, central Japan. Trans Lepid Soc Japan 48: 223–233

Hunter P (2007) The nature of flight. EMBO reports 8: 811–813

Jantzen B, Eisner T (2008) Hindwings are unnecessary for flight but essential for execution of normal evasive flight in Lepidoptera. Proc Natl Acad Sci U S A 105: 16636–16640

Kammer AE (1967) Muscle activity during flight in some large lepidoptera. J Exp Biol 47: 277–295

Kammer AE (1971) The motor output during turning flight in a hawkmoth, *Manduca sexta*. J Insect Physiol 17: 1073–1086

Kanazawa I, Cheng WWW, Pun HSF, Sakiyama Y, Doi H (2015) First migration record of Chestnut Tiger Butterfly, *Parantica sita* niphonica (Moore, 1883) (Lepidoptera: Nymphalidae: Danainae) from Japan to Hong Kong and longest recorded movement by the species. Pan-Pacific Entomologist 91: 91–97

Kutsch W, Stevenson P (1981) Time-correlated flights of juvenile and mature locusts: A comparison between free and tethered animals. J Insect Physiol 27: 455–459

Putney J, Conn R, Sponberg S (2019) Precise timing is ubiquitous, consistent, and coordinated across a comprehensive, spike-resolved flight motor program. Proc Natl Acad Sci U S A 116: 23951–26960

R Core Team (2022) R: A Language and Environment for Statistical Computing. R Foundation for Statistical Computing, Vienna, Austria. URL: https://www.R-project.org/ Accessed 17 March 2024

Ravi S, Crall JD, Fisher A, Combes SA (2013) Rolling with the flow: bumblebees flying in unsteady wakes. J Exp Biol 216: 4299–4309

Reppert SM, Guerra PA, Merlin C (2016) Neurobiology of monarch butterfly migration. Annu Rev Entomol 61: 25–42

Rheuben MB, Kammer AE (1987) Structure and innervation of the 3rd axillary muscle of *Manduca* relative to its role in turning flight. J Exp Biol 131: 373–402

Roeder KD (1951) Movements of the thorax and potential changes in the thoracic muscles of insects during flight. Biol Bull 100: 95–106

Sane SP, Dickinson MH (2001) The control of flight force by a flapping wing: lift and drag production. J Exp Biol 204: 2607–2626

Senda K, Obara T, Kitamura M, Nishikata T, Hirai N, Iima M, et al. (2012a) Modeling and emergence of flapping flight of butterfly based on experimental measurements. Rob Auton Syst 60: 670–678

Senda K, Obara T, Kitamura M, Yokoyama N, Hirai N, Iima M (2012b) Effects of structural flexibility of wings in flapping flight of butterfly. Bioinspir Biomim 7: 025002

Sponberg S, Daniel TL (2012) Abdicating power for control: a precision timing strategy to modulate function of flight power muscles. Proc R Soc London B 279: 3958–3966

Stevenson RD, Josephson RK (1990) Effects of operating frequency and temperature on mechanical power output from moth flight-muscle. J Exp Biol 149: 61–78

Tu MS, Daniel TL (2004) Submaximal power output from the dorsolongitudinal flight muscles of the hawkmoth *Manduca sexta*. J Exp Biol 207: 4651–4662

Wang H, Ando N, Kanzaki R (2008) Active control of free flight manoeuvres in a hawkmoth, *Agrius convolvuli*. J Exp Biol 211: 423–432

Yokoyama N, Senda K, Iima M, Hirai N (2013) Aerodynamic forces and vortical structures in flapping butterfly's forward flight. Phys Fluids 25: 021902

(Received May 18, 2024 / Accepted August 10, 2024 / Published online October 18, 2024)